Increased Macrophage Migration Into Adipose Tissue in Obese Mice

Da Young Oh,[1] Hidetaka Morinaga,[1] Saswata Talukdar,[1] Eun Ju Bae,[2] and Jerrold M. Olefsky[1]

Macrophage-mediated inflammation is a key component of insulin resistance; however, the initial events of monocyte migration to become tissue macrophages remain poorly understood. We report a new method to quantitate in vivo macrophage tracking (i.e., blood monocytes from donor mice) labeled ex vivo with fluorescent PKH26 dye and injected into recipient mice. Labeled monocytes appear as adipose, liver, and splenic macrophages, peaking in 1–2 days. When CCR2 KO monocytes are injected into wild-type (WT) recipients, or WT monocytes given to MCP-1 KO recipients, adipose tissue macrophage (ATM) accumulation is reduced by ~40%, whereas hepatic macrophage content is decreased by ~80%. Using WT donor cells, ATM accumulation is several-fold greater in obese recipient mice compared with lean mice, regardless of the source of donor monocytes. After their appearance in adipose tissue, ATMs progressively polarize from the M2- to the M1-like state in obesity. In summary, the CCR2/MCP-1 system is a contributory factor to monocyte migration into adipose tissue and is the dominant signal controlling the appearance of recruited macrophages in the liver. Monocytes from obese mice are not programmed to become inflammatory ATMs but rather the increased proinflammatory ATM accumulation in obesity is in response to tissue signals.
Diabetes **61:346–354, 2012**

I nsulin resistance is a characteristic feature of patients with type 2 diabetes, and the incidence of type 2 diabetes is rapidly rising in the U.S. (1,2). This is paralleled by an obesity epidemic, and because obesity is the dominant cause of acquired insulin resistance in subjects with type 2 diabetes, or the metabolic syndrome (3,4), it is clear that the obesity epidemic underlies the increasing incidence of type 2 diabetes (5,6). It is well known that obesity leads to a chronic, low-grade tissue inflammatory state that can cause decreased insulin sensitivity (7–9). Therefore, further insight into this chronic inflammatory response is necessary to understand obesity-induced insulin resistance.

Adipose tissue is a key site for this chronic inflammatory response, and this was highlighted by the discovery that increased macrophage content is a feature of adipose tissue from obese mice and humans (10,11). These adipose tissue macrophages (ATMs) secrete a variety of cytokines that can directly cause decreased insulin sensitivity, and the accumulation of ATMs tracks with the degree of obesity and the magnitude of insulin resistance (12–14). Tissue macrophages are derived from circulating monocytes, and

the infiltration of monocytes into tissues is a complex phenomenon involving several steps, including increased expression of adhesion molecules, transmigration of monocytes across the endothelium, migration along a chemotactic gradient into underlying tissues, and, finally, differentiation of monocytes into tissue macrophages (15,16). Therefore, defining the mechanisms underlying monocyte recruitment into adipose tissue in obesity is necessary to understand the mechanism of obesity-mediated insulin resistance.

In the current study, we developed a method for macrophage tracking in vivo, allowing us to measure the ability of circulating monocytes to become tissue macrophages in both lean and obese states. With this approach, circulating monocytes obtained from donor mice are labeled ex vivo with a fluorescent molecule, PKH26. PKH26 is incorporated into the lipid bilayer of cellular membranes and is stable within the cells for 3–4 weeks. The labeled monocytes then are injected into recipient mice, and the appearance of these cells as fluorescently labeled tissue macrophages is monitored by immunohistochemistry and flow cytometry over time, providing a quantitative measure of macrophage tracking.

RESEARCH DESIGN AND METHODS

Animal care and use. Male C57BL/6 mice were fed normal chow (13.5% fat; LabDiet) or a high-fat diet (HFD) (60% fat; Research Diet) ad libitum for 15–20 weeks from 8 weeks of age. CCR2 knockout (KO) and MCP-1 KO mice and wild-type (WT) littermates were provided by Taconic (Hudson, NY). Animals were housed in a specific pathogen-free facility and given free access to food and water. All procedures were approved by the University of California San Diego Animal Care and Use Committee.

Monocyte preparation. Leukocyte pools from C57BL/6 male 12-week-old mice, bled by retro-orbital sinus, were subjected to erythrocyte lysis, and monocyte subsets were enriched with the EasySep mouse monocyte enrichment kit (Stemcell Tech, Vancouver, BC, Canada), following the manufacturer's instructions.

In vitro labeling. Isolated monocytes (5×10^6 to 10×10^6) were washed once in serum-free medium (RPMI-1640) and suspended in 2 mL diluent solution C (included in the PKH26 labeling kit). A total of 2 mL PKH26 (Sigma Chemical, St. Louis, MO) at 2×10^{-3} mol/L in diluent C was added and mixed, and the cells were incubated for 10 min at room temperature in the dark. The staining reaction was halted by the addition of an equal volume (2 mL) of medium supplemented with 10% FBS. The mixture was centrifuged, and the cells were washed once and resuspended in serum-containing medium.

In vivo migration. Subsequent to labeling with PKH26, the monocytes were counted and ~1 × 10^6 viable cells were suspended in 0.2 mL PBS and injected into the femoral vein of the each group of mice. Two days after the injection, the ATMs were immediately isolated from visceral fat tissue and analyzed in the fluorescence-activated cell sorter (FACS).

Confocal microscopy of mouse adipose tissue, liver, and spleen. The method for immunofluorescence study of mouse adipose tissue was followed as described (17). In brief, 2 days after PKH26-labeled monocytes were injected, the mice were killed and slowly perfused by intracardiac injection with 10 mL of 1% paraformaldehyde diluted in PBS. Fingernail-sized fat-pad samples were excised and blocked for 1 h in 5% BSA in PBS with gentle rocking at room temperature. The fat pad was counterstained for 1 h with BODIPY 530/550 C12 (Invitrogen). For the liver and spleen image analysis, tissues were cryopreserved in optimal cutting temperature (OCT) compound and then serially cut

(10 μm) on a cryostat and mounted on gelatin-coated slides. The tissues were imaged on an inverted confocal microscope (Olympus Fluoview 1000).

FACS analysis of macrophages of adipose stromal vascular fraction and liver. Adipocytes and stromal vascular cells were prepared from collagenase-digested adipose tissue, as described previously (18). For liver macrophage analysis, Kupffer cells were prepared by two-step liver collagenase digestion and fractionation on a density gradient, as previously described (19). FACS analysis of stromal vascular cells for macrophage content and subtypes was performed as previously described (18). The antibodies for surface staining were F4/80 (BM8), Ly6C (AL-21), CD11b (M1/70), and CD11c (N418) (eBioscience, San Diego, CA). Numbers obtained were subsequently represented as the percentage of the highest subsets.

RNA isolation and quantitative PCR. Total RNA isolation and quantitative PCR were performed as described previously (20). Gene expression levels were calculated after normalization to the standard housekeeping genes *RPS3* and *GAPDH* using the $\Delta\Delta C_T$ method (20) and expressed as relative mRNA levels compared with internal control. Primer information is available upon request.

Bromodeoxyuridine labeling of proliferating cells in vivo. Mice were injected intraperitoneally with 100 μL of 10 mg/mL bromodeoxyuridine (BrdU) in Dulbecco's PBS 24 and 3 h before the experimental end point.

Data analysis. The values presented are expressed as the means ± SEM. The statistical significance of the differences between various treatments was determined by one-way ANOVA with the Bonferroni correction using GraphPad Prism 5.0 (San Diego, CA). $P < 0.05$ was considered significant.

RESULTS

Studies of macrophage tracking. ATMs play a key role in orchestrating the insulin resistance associated with obesity (7–11). Activated, proinflammatory ATMs secrete cytokines, which can have local paracrine effects or systemic endocrine effects to cause decreased insulin sensitivity (12–14,16). Therefore, understanding the in vivo mechanisms governing the conversion of circulating monocytes to ATMs is an important goal. To this end, we have developed a method for in vivo macrophage tracking. With this approach, peripheral blood monocytes (PBMs) are isolated from donor mice and fluorescently labeled ex vivo by incubation with PKH26 (red) for 15 min. The fluorescently labeled cells then are injected into recipient mice, and the appearance of these injected monocytes as tissue macrophages is monitored (Fig. 1A). To track monocytes into ATMs, adipose tissue is obtained and the stromal vascular fraction (SVF) is isolated, followed by FACS analysis to quantitate total and fluorescently labeled ATMs. Immunofluorescence microscopy is used to track monocytes into liver and spleen. As seen in Fig. 1B, the injected monocytes are rapidly cleared from circulation within several hours, and, by 6 h, labeled macrophages can be detected in adipose tissue by FACS analysis of SVFs, as well as immunofluorescence microscopy (Fig. 1C). By 2 days, ~10% of the total ATMs are fluorescently labeled, indicating their origin from the originally injected labeled monocytes (Fig. 1D). A much larger proportion of labeled cells appear in the liver and spleen, as seen by flow cytometry (Fig. 1D) and immunofluorescence microscopy (Fig. 1E).

The role of CCR2 and MCP-1 in macrophage recruitment. Monocytes migrate into tissues in response to chemotactic signals, and, therefore, we examined the role of the CCR2/MCP-1 system in this process. In peripheral blood, CCR2 expression is largely limited to monocytes and some T cells (21), and it is known that the ability of CCR2-deficient mice to recruit monocytes to sites of inflammation is impaired (22). To test these concepts in our system, we labeled PBMs derived from WT and CCR2 KO donor mice and injected them into obese WT recipients (Fig. 2A). In complementary experiments, we injected WT fluorescently labeled donor monocytes into obese WT or

MCP-1 KO recipients (Fig. 2D). As seen in Fig. 2B and C, when the chemokine receptor, CCR2, is deleted from the labeled donor monocytes, an ~40% decrease in labeled ATM accumulation occurs. Of interest, there is a much greater decrease in monocyte recruitment to liver. Quite comparable results were seen when labeled WT monocytes were injected into MCP-1 KO mice. These results demonstrate the importance of the CCR2/MCP-1 system in macrophage recruitment and indicate that in our system the injected fluorescently labeled monocytes behave in the expected manner. Of interest, CCR2/MCP-1 seems to be a much more dominant chemokine with respect to macrophage tracking to liver compared with adipose tissue. Although CCR2/MCP-1 is important for ATM accumulation, deletion of these molecules only decreases macrophage recruitment to adipose tissue by ~40%, indicating that there are one or more additional chemotactic signals that are key to this process.

Macrophage tracking in lean and obese mice. Increased ATM accumulation has been extensively described in insulin-resistant, obese states, but the precise mechanism for this remains to be determined. One important question is whether circulating monocytes from lean or obese mice are preprogrammed for their subsequent behavior as ATMs. In other words, are monocytes from obese mice predestined to confer increased proinflammatory ATMs, or is the macrophage content of adipose tissue in lean versus obese mice strictly a function of tissue cues. To explore these questions, we isolated PBMs from chow-fed lean mice or HFD-fed obese mice, labeled them with PKH26 fluorescent dye, and then injected the labeled monocytes into either lean or obese recipients. As seen in Fig. 3A and B, FACS analysis and gene expression for various monocyte and macrophage surface markers indicate that PBMs from lean or obese donors appear similar, including no differences in expression of *CCR2*. The only differences were a small secondary peak of Ly6C high monocytes and an increased expression of *CD68* in the donor cells from obese mice. As seen in Fig. 3C, labeled macrophage accumulation peaks at ~2–3 days and then gradually declines. Of importance, there is a dramatic increase in the number of macrophages appearing in obese adipose tissue compared with lean tissue (Fig. 3D). In addition, the subsequent decline in labeled ATM content up to 21 days is greater in the lean mice (Fig. 3C).

The four-way experiment is depicted in Fig. 3E–G. These results demonstrate that when donor cells from lean or obese mice are injected into lean recipients, a low level of labeled ATMs is seen. Conversely, when monocytes from lean or obese mice are injected into obese recipients, a much greater and comparable increase in labeled ATM accumulation occurs. These results indicate that the PBMs are naive to their ultimate fate, with respect to ATM accumulation, and that monocytes from lean or obese mice behave in the same manner after injection. Thus, independent of the donor mice, the increased ATM accumulation in obesity is a function of signals from the recipient animals.

Properties of labeled ATMs. Previous studies have shown that the CD11c$^+$ subpopulation of macrophages comprises the majority of the increased ATM content in obesity (18,23). When the newly recruited labeled ATMs were analyzed by FACS analysis, we found (Fig. 4B) that 80–90% of the labeled ATMs were CD11c$^+$ (Fig. 4A) in the obese animals, whereas only ~20% were CD11c$^+$ in the lean group. This same concept is seen when comparing
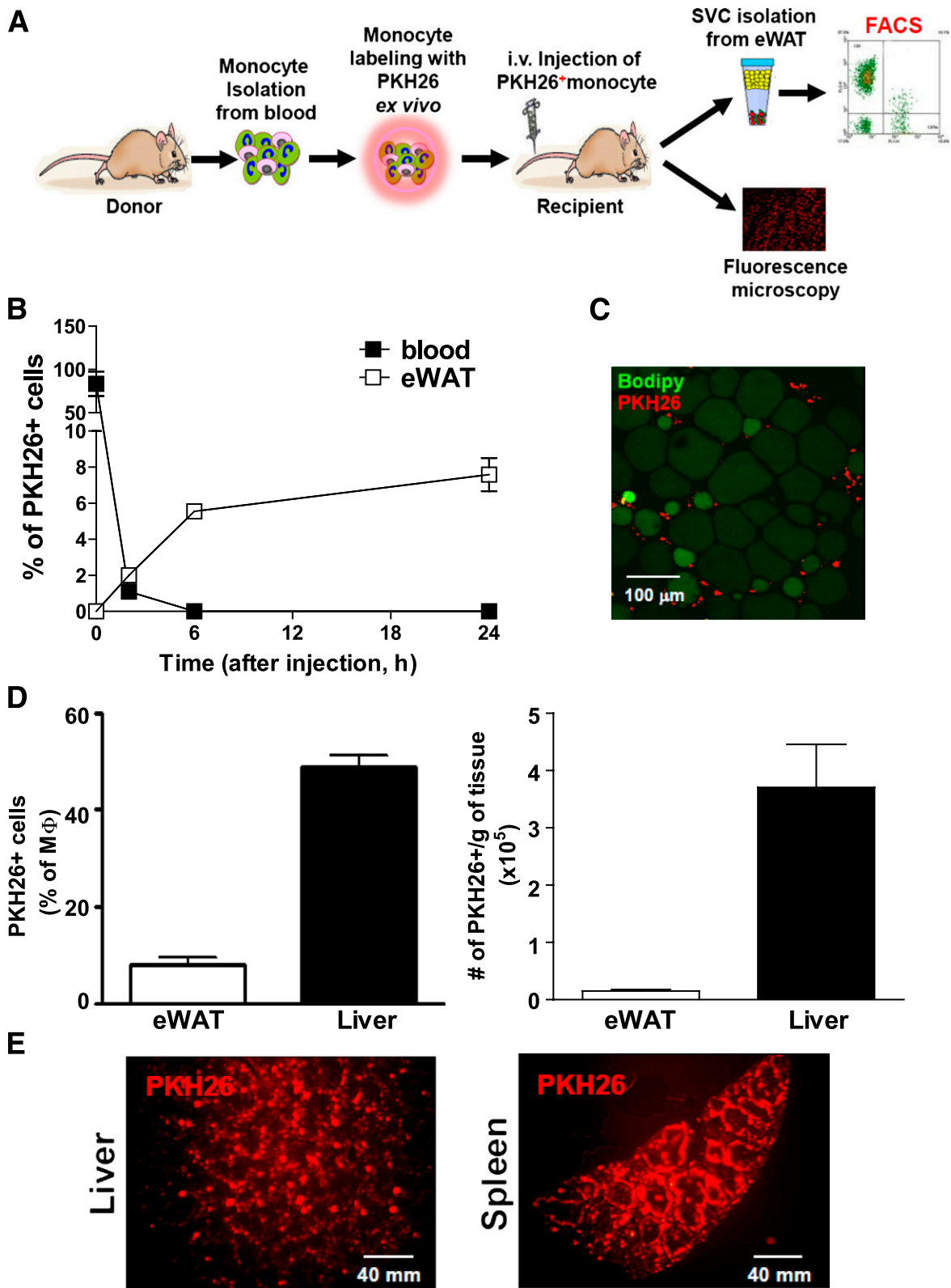
FIG. 1. Monocyte tracking with PKH26 fluorescent labeling. *A*: Schematic diagram of the monocyte-tracking strategy. *B*: The time course of clearance of PKH26-labeled monocytes from circulating blood (■) and appearance in eWAT (plotted as the percentage of SVF; □) from lean mice. Data are means ± SEM of three mice per each time point from two independent experiments. *C*: Immunohistochemistry of PKH26-labeled mono-cytes in adipose tissue observed by confocal microscope. Red cells are PKH26^{+} ATMs located around green adipocytes. The image is representative of similar results from three to four independent experiments. Scale bar represents 100 μm. *D*: PKH26^{+} cells were plotted as the percentage of the total macrophage number (*left graph*) in lean mice adipose tissue (eWAT) and liver and total PKH26^{+} cells per gram of tissue (*right graph*). Results are pooled data from four independent experiments. *n* = ~7–8. *E*: Immunohistochemistry analysis of liver and spleen after PKH26-labeled monocyte injection. The image is representative of similar results from three to four independent experiments. Scale bar represents 40 mm. (A high-quality digital representation of this figure is available in the online issue.)
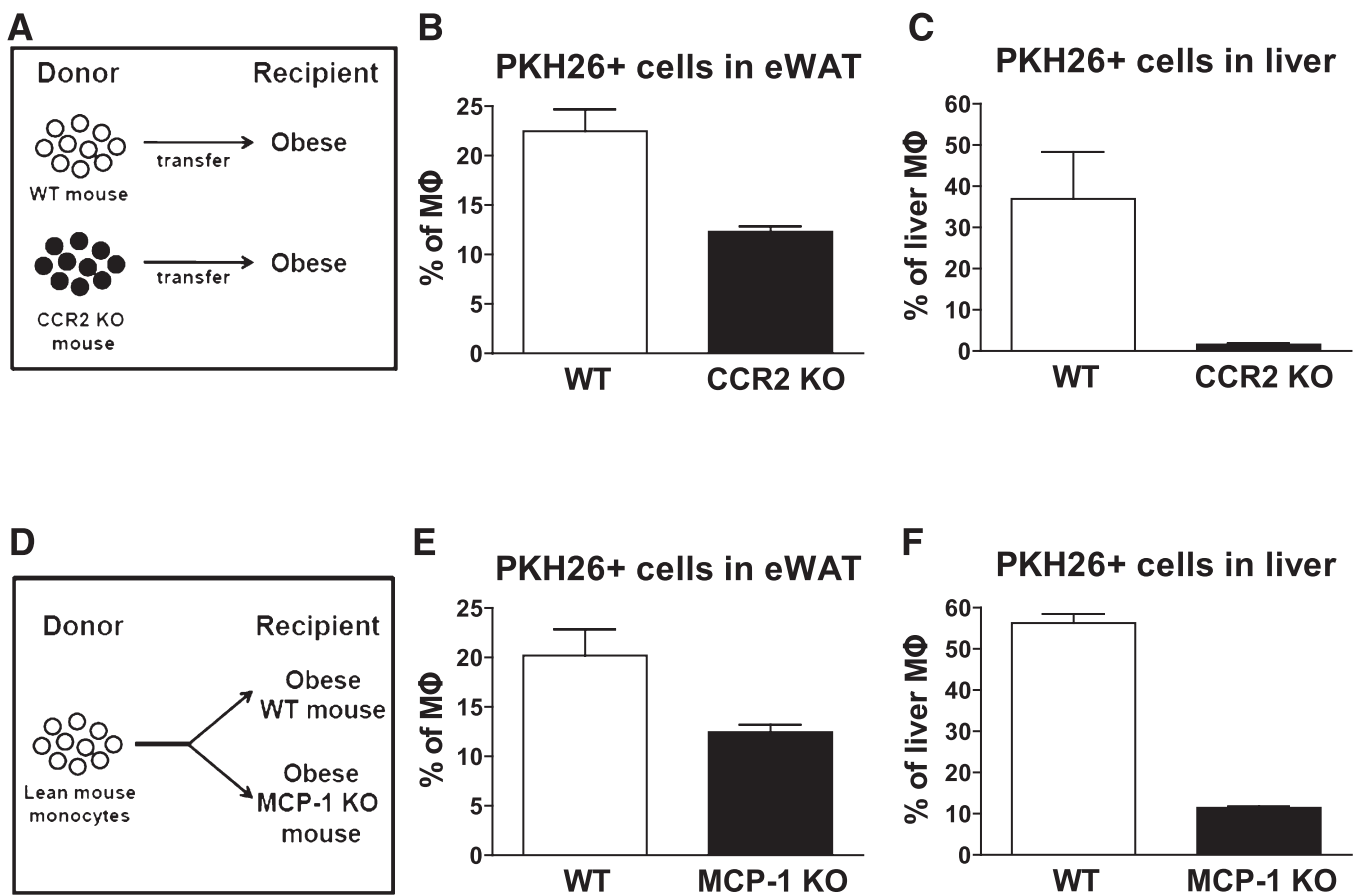
FIG. 2. Impaired monocyte recruitment with CCR2 monocytes and in MCP-1 KO mice. *A*: Blood monocytes were prepared from WT and CCR2 KO mice and then injected to HFD-fed/obese recipient mice. The number of PKH26^{+} cells in eWAT (*B*) and liver (*C*) were analyzed by a FACS and then plotted as the mean ± SEM from three independent experiments. *n* = 6 in each group. *D*: Monocytes were isolated from lean WT mice and, labeled with PKH26, injected into either obese WT or MCP-1 KO mice. The number of PKH26^{+} cells in eWAT (*E*) and liver (*F*) were analyzed by a FACS and then plotted as the mean ± SEM from three independent experiments. *n* = 5 in each group.

Fig. 3*F* and *G*. This demonstrates that not only are there increased ATMs in obesity, but there is a marked shift in macrophage subpopulations, favoring the M1-like, proinflammatory, CD11c^{+} macrophage phenotype. Thus, in obesity, the great majority of monocytes that migrate into adipose tissue become CD11c^{+} ATMs.

Because circulating monocytes are CD11c^{−} (24) (Fig. 3*A*), the acquisition of CD11c positivity by ATMs must involve differentiation of newly recruited monocytes into M1-like CD11c^{+} macrophages. As seen in time-course studies, at 1–2 days postinjection the labeled ATMs in the HFD-fed/obese mice are roughly equally divided into CD11c^{+} versus CD11c^{−} populations (Fig. 4*B*). However, over the subsequent 2 weeks, an increasing proportion of these ATMs became CD11c^{+}, accompanied by a marked decrease in the CD11c^{−} population, such that by 14 days, 85% of the labeled ATMs are CD11c. This indicates the plasticity of freshly recruited ATMs, showing that they gradually transform into the proinflammatory, M1-like CD11c^{+} phenotype characteristic of established obesity. Although the mechanisms of this transdifferentiation remain to be identified, it is most likely a response to local signals emanating from obese adipose tissue, because this process did not occur in the lean animals (Fig. 4*A*).

Independent of labeled monocyte administration, if one examines ATM content in uninjected lean versus obese mice, the results show the expected increase in ATM content along with the well-described marked increase in the population of proinflammatory CD11c^{+} (M1-like) ATMs (Fig. 4*C*). In the lean state, the great majority of ATMs are CD11c^{−}, and there is a modest increase in this macrophage subpopulation in the obese state, so that in established obesity, ~60% of the ATMs are CD11c^{−} (Fig. 4*C*). Because ~90% of the freshly recruited monocyte-derived ATMs are CD11c^{+}, this raises the question as to the origin of the resident CD11c^{−} ATMs. Recent studies have shown that these M2-like macrophages have a high proliferative capacity (25). Thus, accumulation in adipose tissue could reflect either a low rate of migration into adipose tissue, coupled with a high degree of postresidency proliferation, or perhaps origination from a cell type other than circulating monocytes.

It is of interest that although the bulk of the labeled monocytes are cleared from circulation within several hours, labeled ATM content continues to rise for at least 48 h. This could be attributed to a low level of ongoing recruitment of new macrophages over this time period or to proliferation of the initial cohort of recruited monocytes. To assess this, we performed in vivo BrdU labeling and immunohistochemistry of Ki67 as measures of cellular proliferation. As seen in Fig. 4*D*, ~25% of ATMs are PKH26^{+}, but only a small fraction (~2%) of these cells also were positive for BrdU. A similar low proportion (~5%) of cells stained positive for Ki67 (Fig. 4*E*). These findings suggest that ongoing recruitment
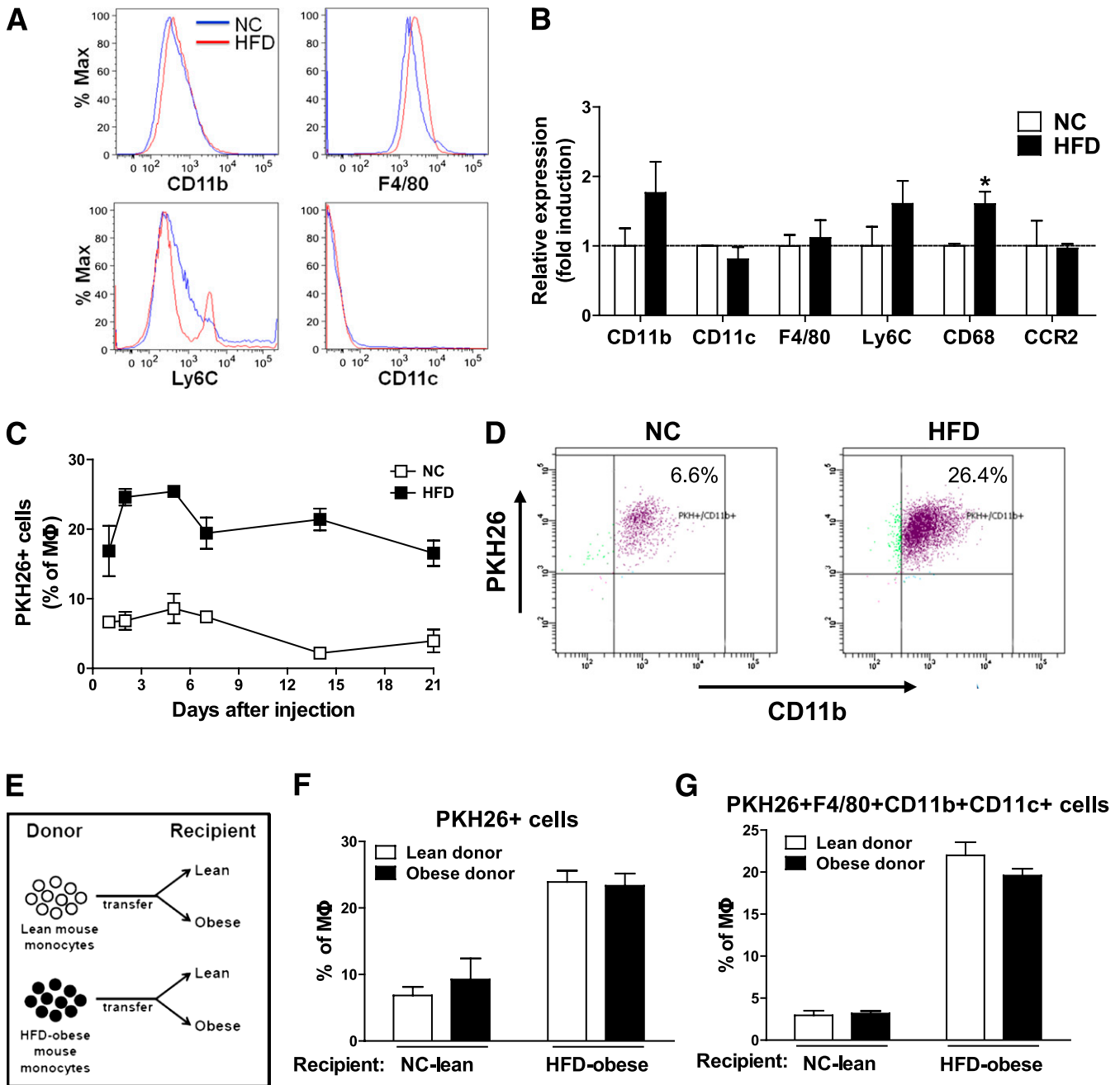
FIG. 3. Quantitation of monocyte migration in lean and obese mice. *A*: Comparison of indicated monocyte markers in blood monocytes obtained from normal chow (NC)/lean and HFD-fed/obese mice. This was a representative plot for each marker from three independent experiments. *n* = ~5–6 in each group. *B*: Relative mRNA levels for indicating genes in the monocytes from an NC/lean and HFD-fed/obese mouse, as measured by quantitative PCR. Data are expressed as the mean ± SEM of three independent experiments in triplicate. *P < 0.05. *n* = 5 per group. *C*: Time course of appearance of injected monocytes as ATMs in recipient NC/lean or HFD-fed/obese recipient mice. Data present the mean ± SEM of three mice for each time point from three independent experiments. *D*: Two days after labeled monocyte injection into lean vs. obese mice, PKH26$^+$ cells were calculated from total F4/80$^+$ATMs by FACS analysis and then plotted with CD11b$^+$ fluorescence. The scattergram is representative of five to six independent mice from each group. *E*: Donor mice were lean or obese, and labeled cells were injected into lean or obese recipients. After injection, PKH26$^+$-labeled monocytes (*F*) and PKH26$^+$F4/80$^+$CD11b$^+$CD11c$^+$ cells (*G*) were tracked and plotted as the percentage of total macrophages in adipose tissue. The results were analyzed by a FACS and then plotted as the mean ± SEM from more than three independent experiments. *n* = 6 in each group.

of new monocytes, at least in part, underlies the increase in labeled ATM content 12 h after the injection.

DISCUSSION

The accumulation of tissue macrophages, particularly in adipose tissue, is a defining feature of the chronic, low-grade inflammatory state in obesity (7–15). The CD11c$^+$, M1-like, macrophage subpopulation represents the majority of the excess ATMs in obesity (18,23). These macrophages are highly proinflammatory, releasing an array of cytokines/chemokines that can cause decreased insulin sensitivity through paracrine and endocrine mechanisms (13,14,23). A better understanding of the events that lead to ATM accumulation in obesity will sharpen our pathophysiologic knowledge concerning the mechanisms of
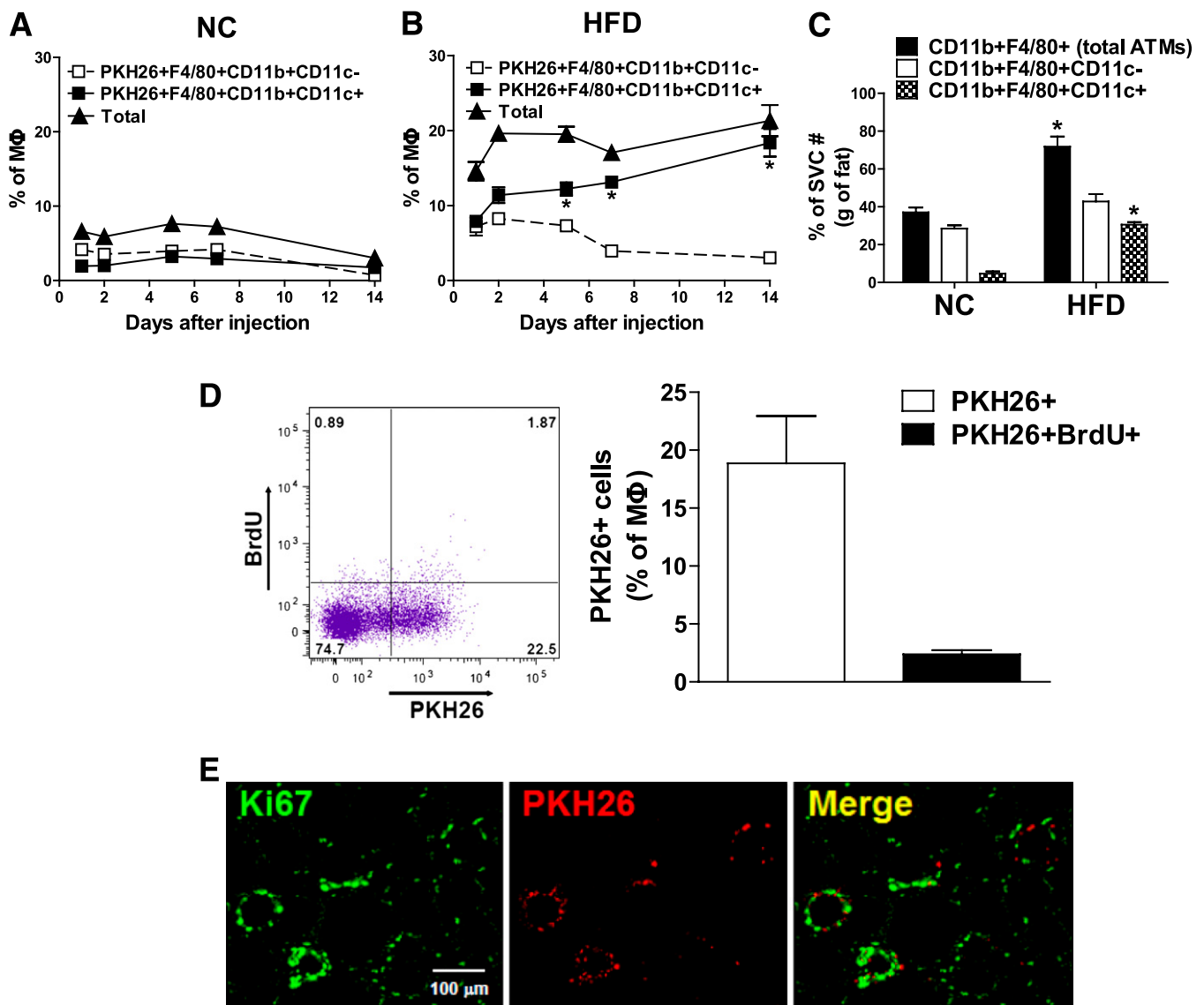
FIG. 4. Properties of monocyte-derived ATMs. Differentiation of injected monocytes into inflammatory ATMs was analyzed as CD11c$^+$ vs. CD11c$^-$ ATMs in NC/lean (A) and HFD-fed/obese (B) mice at the indicated times and then plotted as the mean ± SEM from three independent experiments. n = ~8–9 in each group. C: The increase in triply positive cells accounts for the majority of the increase in total ATMs. The numbers of cells of total ATMs (CD11b$^+$F4/80$^+$), doubly positive (F4/80$^+$CD11b$^+$CD11c$^-$), and triply positive (F4/80$^+$CD11b$^+$CD11c$^+$) cells were calculated from FACS data and SVF cell counts and expressed per gram of eWAT. n = 6 per group. *P < 0.05 vs. NC. Data are means ± SEM. D: To detect proliferation of PKH26-labeled monocytes, the proliferation marker BrdU was injected twice at 24 and 3 h before the end point experiment at day 7 after PKH26$^+$ cell injection. PKH26$^+$ and PKH26$^+$ BrdU$^+$ ATMs were analyzed by a FACS (left) and then plotted as the mean ± SEM from three independent experiments (right). n = 6. The scattergram is representative of five to six independent mice. E: Immunohistochemistry analyses of the proliferation marker, Ki67, to detect proliferation of PKH26$^+$ ATMs in adipose tissue. The image is representative of similar results from three to four independent experiments. Scale bar represents 100 μm. (A high-quality digital representation of this figure is available in the online issue.)

inflammation and insulin resistance and may guide strategies for future therapeutic interventions. In the current studies, we have developed an in vivo method to track circulating monocytes as they become tissue macrophages. With this method, circulating monocytes are prepared from a donor animal, labeled ex vivo with fluorescent dye, and then injected into a recipient animal. The appearance of the labeled monocytes as tissue macrophages then is monitored over time by immunohistochemistry and flow cytometry. We show that circulating monocytes have a relatively short half-life (several hours) in blood and rapidly appear as tissue macrophages and that this process is at least partially dependent on the CCR2/MCP-1 system. In this context, an important question we attempted

to address is "Where do the signals that lead to increased ATM content originate?" Because increased fluorescent ATM accumulation occurred in obese recipient mice, regardless of whether donor monocytes were derived from lean or obese animals, our data lead to the conclusion that, in obesity, the circulating monocyte is not preprogrammed or destined to become an activated tissue macrophage and that the information governing this process is derived from recipient tissues.

After injection into recipient mice, the fluorescently labeled monocytes are cleared from the circulation within several hours and subsequently can be readily detected in adipose tissue, liver, and spleen. In lean animals, adipose tissue accumulation peaks at 1–2 days, remains stable for

~1 week, and gradually declines over the next 2 weeks. In obese recipients, there is a much larger increase in labeled ATMs, peaking at 2 days, with levels remaining relatively constant for at least 2–3 weeks. As expected, a sizable number of labeled cells appear in the spleen, and, interestingly, a substantial influx of macrophages was detected in the liver. These latter cells are distinct from Kupffer cells and represent newly recruited hepatic macrophages (RHMs). Per gram of tissue, there were approximately three times as many RHMs as ATMs.

The rather large number of macrophages that accumulate in the liver is of interest and a bit surprising. Possible explanations might be that the fluorescently labeled monocytes are injected intravenously and are, therefore, naturally directed to the liver because of the high rate of hepatic blood flow and the fenestrated endothelium within hepatic sinusoids. However, the fact that this migration into the liver is largely inhibited by CCR2 or MCP-1 deletion indicates that it is a physiologic process subject to appropriate regulation. The itinerary of circulating monocytes prior to liver uptake is likely a somewhat complicated process that is not fully understood at this point. As just one example, it seems quite probable that all the labeled monocytes that end up in the liver do not arrive by first-passage uptake of the injected cells. As shown in Fig. 1E, a fair number of injected monocytes are taken up by the spleen, which is a known storage site for monocytes and other immune cells. It seems likely that reemergence of monocytes from the spleen back into the bloodstream or lymphatics can lead to recirculation to the liver in response to tissue cues. It is clear that more information is needed to fully understand this process.

With respect to tracking of the fluorescently labeled monocytes to adipose tissue, again, prior to chemotaxis into adipose tissue, the monocyte trafficking pattern is likely to be more involved than simple first-passage uptake of the intravenously injected cells. For example, the data presented do not precisely quantitate the half-life, or residence time, of a macrophage in adipose tissue. Thus, our results do not determine whether the ATMs that are present in adipose tissue at 1–2 weeks are the same cells that were there after 2 days. It certainly is possible that some ATMs that migrate into adipose tissue undergo apoptosis/necrosis or exit the tissue in some other way, followed by some degree of repopulation by labeled monocytes derived from a storage site, such as the spleen.

Several reports have suggested that specific subpopulations of circulating monocytes, characterized as Ly6C^{hi}, have an increased propensity to become arterial wall macrophages and foam cells in the etiology of atherosclerosis (24,26,27). With this concept, a degree of predetermination already is present in the circulating monocyte before it becomes a foam cell. To determine whether a similar process might exist with respect to ATM accumulation in obesity, we administered labeled monocytes from lean or obese donors into either lean or HFD-fed/obese recipient animals. The isolated monocytes from the lean and obese groups appeared similar, with the exception of a small second peak of Ly6C high monocytes in the obese donor cells. More importantly, as seen in Fig. 3, monocytes derived from lean or obese mice behaved identically, with respect to their appearance, as ATMs. Thus, when monocytes from lean or obese mice were injected into lean recipients, a low amount of ATM accumulation occurred. When the two groups of monocytes were injected into obese mice, a comparable several-fold increase in ATM

content was observed. Thus, in obesity, monocytes migrate more rapidly and to a greater extent into adipose tissue to become ATMs. From these studies, we conclude that circulating monocytes from obese mice are not preprogrammed to become inflammatory tissue macrophages and that the signals responsible for the increased ATM content in obesity largely are derived from tissue sources.

It is possible that the injected monocytes expand the circulating monocyte pool sufficiently to increase monocyte uptake into liver and adipose tissue by mass action. However, based on our calculations, we believe such an effect, if it exists, would be modest. Thus, we injected $0.5 - 1 \times 10^6$ cells into a given recipient mouse, and the endogenous pool of circulating monocytes in a lean chow-fed mouse is ~10^6 cells and in the HFD-fed mouse is ~3×10^6 (attributed to the well-known HFD-induced monocytosis). Therefore, to the extent that expansion of the monocyte pool drives monocyte tissue migration in these experiments, such an effect would minimize rather than exaggerate the differences we observed, because this would be greater in the lean chow-fed mice compared with the HFD-fed/obese mice, whereas we found greater ATM accumulation in the obese mice. Furthermore, recirculation of the labeled monocyte from the spleen would mitigate any effects of immediate expansion of circulating monocyte pools as a result of the injection. To the extent that immediate postinjection expansion of the circulating monocyte pool contributes to increased labeled ATM accumulation, one would predict a higher total number of ATMs (labeled + unlabeled) in injected compared with noninjected mice. When we measured total ATM number per gram epididymal white adipose tissue (eWAT) in noninjected mice, the values are $(0.41 \pm 0.07) \times 10^6$ in chow-fed animals and $(1.25 \pm 0.20) \times 10^6$ in HFD-fed mice. In the injected recipient mice, the corresponding values are $(0.60 \pm 0.24) \times 10^6$ vs. $(1.40 \pm 0.44) \times 10^6$. Thus, although it is possible that some component of the labeled macrophage appearance in liver and adipose tissue is attributed to immediate expansion of the circulating monocyte pool, we think such an effect would be modest and would tend to underestimate the differences we have observed.

The signals that lead to macrophage migration are tissue chemokines that can be released by adipocytes, hepatocytes, and, perhaps other cell types (16,27–29). Furthermore, once the initial wave of macrophages arrives in the tissue, these cells can release their own chemotactic signals, causing a further influx of monocytes, leading to a positive, feed-forward process. Because a number of previous reports have demonstrated the importance of MCP-1 as a chemotactic signal for monocyte migration into adipose tissue (30), we used our fluorescently labeled monocyte-tracking technique to quantitate the importance of the CCR2/MCP-1 axis in the appearance of RHMs and ATMs. When labeled monocytes from CCR2 KO mice were injected into WT recipients, or labeled WT monocytes were injected into MCP-1 KO mice, an ~40% reduction in ATM content was observed. This indicates the importance of the CCR2/MCP-1 system for the recruitment of monocytes into adipose tissue but also indicates that other chemotactic signals are operative and could account for the majority of the monocyte influx. In contrast, deletion of the CCR2/MCP-1 system led to an ~85% decrease in RHMs, demonstrating the dominance of MCP-1 as the chemotactic signal in liver. Thus, the mixture of chemotactic signals responsible for ATM accumulation in obesity is more complex than the more

monotonic dependence of RHM migration on the CCR2/MCP-1 system.

Our functional in vivo studies revealed another dynamic feature about ATM biology. The appearance of labeled ATMs in the obese mice peaked at 2 days, and, at that time, ~50% of the labeled cells displayed the CD11c$^+$, M1-like phenotype. At 14 days postinjection, the total number of ATMs was relatively unchanged, but at this point, ~95% of the cells were CD11c$^+$. At the same time, fewer cells were CD11c$^-$. These data indicate that after the initial transformation of postmigratory monocytes to ATMs, they progressively polarized toward the M1-like, CD11c$^+$ state. These data indicate that ATMs retain a degree of plasticity so that within adipose tissue, they can polarize toward a particular phenotype, depending on the tissue cues within the adipose depot.

It is of interest that in established obesity, at least one-half of the ATMs are CD11c$^-$ (18) (Fig. 4C), whereas our studies show that >90% of the newly recruited fluorescently labeled monocytes end up as CD11c$^+$ ATMs. This raises the question as to the origin of the CD11c$^-$ ATMs in obesity. In this regard, Jenkins et al. (25) have reported that M2-like, alternatively activated, recruited ATMs retain a high proliferative capacity within the tissue compared with M1-like ATMs. Integrating the results of Jenkins et al. together with our current data on in vivo macrophage tracking suggests the idea that CD11c$^+$, M1-like ATMs in obesity are largely derived from circulating monocytes recruited to the adipose tissue in response to tissue-derived chemokine signals. In contrast, the large number of CD11c$^-$ ATMs present in obese adipose tissue may reflect either a low rate of monocyte recruitment coupled with a high proliferative capacity of those cells destined for the alternatively activated phenotype. Another possibility is that the resident alternatively activated, M2-like, CD11c$^-$ ATMs may be derived from a cell type other than circulating monocytes. Clearly, additional work will be required to resolve these possibilities. Consistent with this idea, we also found that ATMs displayed a limited degree of proliferation within adipose tissue but that proliferation was ~2.5-fold greater in the CD11c$^-$ compared with CD11c$^+$ ATMs. Thus, using both BrdU and Ki67 labeling, we found that ~10% of the fluorescent ATMs were positive for these markers of cell division. Taken together, these results indicate that during established obesity, the number of proinflammatory, CD11c$^+$, M1-like ATMs is a result of increased monocyte migration into adipose tissue, polarization of ATMs toward the M1-like state, and a low level of proliferation of these cells after they become ATMs.

REFERENCES

1. Olefsky JM, Courtney CH. Type 2 diabetes mellitus: etiology, pathogenesis, and natural history. In *DeGroot Textbook of Endocrinology.* 5th ed. Philadelphia, W.B. Saunders and Company, 2005, p. 1093–1117
2. Reaven GM. The insulin resistance syndrome: definition and dietary approaches to treatment. Annu Rev Nutr 2005;25:391–406
3. Després JP, Lemieux I. Abdominal obesity and metabolic syndrome. Nature 2006;444:881–887
4. Haffner S, Taegtmeyer H. Epidemic obesity and the metabolic syndrome. Circulation 2003;108:1541–1545
5. Ford ES, Williamson DF, Liu S. Weight change and diabetes incidence: findings from a national cohort of US adults. Am J Epidemiol 1997;146: 214–222
6. Resnick HE, Valsania P, Halter JB, Lin X. Relation of weight gain and weight loss on subsequent diabetes risk in overweight adults. J Epidemiol Community Health 2000;54:596–602
7. Heilbronn LK, Campbell LV. Adipose tissue macrophages, low grade inflammation and insulin resistance in human obesity. Curr Pharm Des 2008; 14:1225–1230
8. Schenk S, Saberi M, Olefsky JM. Insulin sensitivity: modulation by nutrients and inflammation. J Clin Invest 2008;118:2992–3002
9. Shoelson SE, Lee J, Goldfine AB. Inflammation and insulin resistance. J Clin Invest 2006;116:1793–1801
10. Weisberg SP, McCann D, Desai M, Rosenbaum M, Leibel RL, Ferrante AW Jr. Obesity is associated with macrophage accumulation in adipose tissue. J Clin Invest 2003;112:1796–1808
11. Xu H, Barnes GT, Yang Q, et al. Chronic inflammation in fat plays a crucial role in the development of obesity-related insulin resistance. J Clin Invest 2003;112:1821–1830
12. Fantuzzi G. Adipose tissue, adipokines, and inflammation. J Allergy Clin Immunol 2005;115:911–919; quiz 920
13. Tilg H, Moschen AR. Adipocytokines: mediators linking adipose tissue, inflammation and immunity. Nat Rev Immunol 2006;6:772–783
14. Shoelson SE, Lee J, Yuan M. Inflammation and the IKK beta/I kappa B/NF-kappa B axis in obesity- and diet-induced insulin resistance. Int J Obes Relat Metab Disord 2003;27(Suppl. 3):S49–S52
15. Curat CA, Miranville A, Sengenès C, et al. From blood monocytes to adipose tissue-resident macrophages: induction of diapedesis by human mature adipocytes. Diabetes 2004;53:1285–1292
16. Baggiolini M. Chemokines and leukocyte traffic. Nature 1998;392:565–568
17. Lumeng CN, DelProposto JB, Westcott DJ, Saltiel AR. Phenotypic switching of adipose tissue macrophages with obesity is generated by spatiotemporal differences in macrophage subtypes. Diabetes 2008;57: 3239–3246
18. Nguyen MT, Favelyukis S, Nguyen AK, et al. A subpopulation of macrophages infiltrates hypertrophic adipose tissue and is activated by free fatty acids via Toll-like receptors 2 and 4 and JNK-dependent pathways. J Biol Chem 2007;282:35279–35292
19. Nnalue NA, Shnyra A, Hultenby K, Lindberg AA. Salmonella choleraesuis and Salmonella typhimurium associated with liver cells after intravenous inoculation of rats are localized mainly in Kupffer cells and multiply intracellularly. Infect Immun 1992;60:2758–2768
20. Yoshizaki T, Milne JC, Imamura T, et al. SIRT1 exerts anti-inflammatory effects and improves insulin sensitivity in adipocytes. Mol Cell Biol 2009; 29:1363–1374
21. Mack M, Cihak J, Simonis C, et al. Expression and characterization of the chemokine receptors CCR2 and CCR5 in mice. J Immunol 2001;166:4697–4704

22. Weisberg SP, Hunter D, Huber R, et al. CCR2 modulates inflammatory and metabolic effects of high-fat feeding. J Clin Invest 2006;116:115–124

23. Lumeng CN, Bodzin JL, Saltiel AR. Obesity induces a phenotypic switch in adipose tissue macrophage polarization. J Clin Invest 2007;117:175–184

24. Yona S, Jung S. Monocytes: subsets, origins, fates and functions. Curr Opin Hematol 2010;17:53–59

25. Jenkins SJ, Ruckerl D, Cook PC, et al. Local macrophage proliferation, rather than recruitment from the blood, is a signature of TH2 inflammation. Science 2011;332:1284–1288

26. Woollard KJ, Geissmann F. Monocytes in atherosclerosis: subsets and functions. Nat Rev Cardiol 2010;7:77–86

27. Tacke F, Alvarez D, Kaplan TJ, et al. Monocyte subsets differentially employ CCR2, CCR5, and CX3CR1 to accumulate within atherosclerotic plaques. J Clin Invest 2007;117:185–194

28. Anderson EK, Gutierrez DA, Hasty AH. Adipose tissue recruitment of leukocytes. Curr Opin Lipidol 2010;21:172–177

29. Sell H, Eckel J. Chemotactic cytokines, obesity and type 2 diabetes: in vivo and in vitro evidence for a possible causal correlation? Proc Nutr Soc 2009;68:378–384

30. Kamei N, Tobe K, Suzuki R, et al. Overexpression of monocyte chemo-attractant protein-1 in adipose tissues causes macrophage recruitment and insulin resistance. J Biol Chem 2006;281:26602–26614